We are IntechOpen, the world's leading publisher of Open Access books Built by scientists, for scientists

6,900
Open access books available

186,000
International authors and editors

200M
Downloads

Our authors are among the

154
Countries delivered to

TOP 1%
most cited scientists

12.2%
Contributors from top 500 universities

CLARIVATE ANALYTICS
BOOK CITATION INDEX
INDEXED

WEB OF SCIENCE™

Selection of our books indexed in the Book Citation Index
in Web of Science™ Core Collection (BKCI)

Interested in publishing with us?
Contact book.department@intechopen.com

Numbers displayed above are based on latest data collected.
For more information visit www.intechopen.com

Food Chilling Methods and CFD Analysis of a Refrigeration Cabinet as a Case Study

Radu Roşca, Ioan Țenu and Petru Cârlescu

Additional information is available at the end of the chapter

http://dx.doi.org/10.5772/intechopen.69136

Abstract

This chapter presents the most significant facts about food chilling. For food chilling, the chilling medium in mechanically cooled chillers may be air, water or another secondary cooling agent (slurry ice), or metal surfaces (heat exchangers). Ice chilling is also presented. CFD simulation is applied to a vertical display cabinet with four shelves. In order to evaluate the temperature gradient, the following stages are taken into account: preprocessing—geometry set-up and design of the discretization scheme; processing—introduction of the boundary conditions and calculation; and post-processing—visualization of the velocity and temperature fields.

Keywords: chilling equipment, secondary agents, refrigeration cabinet, CFD simulation

1. Introduction

Refrigeration slows down the chemical and biological processes in foods, such as the accompanying deterioration and the loss of quality, extending the shelf life of the products, with minimum changes to the sensory characteristics and nutritional properties.

Temperatures in the range of 0–5°C slow down the development and growth of microorganisms, but some pathogenic agents can grow to large numbers at these temperatures or are still sufficiently virulent to cause poisoning. Because the activity of most of the pathogenic agents is only slowed down and not stopped, long-term storage of refrigerated products can finally

cause food poisoning [1]. In these cases, when a longer preservation period is needed, freezing must be used to minimize any physical, biochemical, and microbiological changes affecting quality during storage. The storage life of fresh perishable foods, such as meats, fish, fruits, and vegetables, can be extended by several days by cooling, and by several weeks or months by freezing [2, 3]. During freezing, most of the water content of the meat, about 80%, solidifies into pure ice crystals, accompanied by a separation of dissolved solids [2, 4].

Chilled foods are commonly grouped into three categories, according to the storage temperature range [1]:

- −1 to +1°C—fresh fish, meats, sausages and ground meats, smoked meats, and breaded fish;

- 0 to +5°C—pasteurized canned meat, milk, cream, yoghurt, prepared salads, sandwiches, baked goods, fresh pasta, fresh soups and sauces, pizzas, pastries, and unbaked dough;

- 0 to +8°C—fully cooked meats and fish pies, cooked or uncooked cured meats, butter, margarine, hard cheese, cooked rice, fruit juices, and soft fruits.

In order to chill fresh foods, it is necessary to remove the sensible heat and also the heat generated by the respiratory activity of vegetables and fruits; in animal tissues, aerobic respiration rapidly declines when the supply of oxygenated blood is stopped at slaughter [1, 4].

2. Cooling rate and duration

Cooling rate may be defined as [4]:

$$w = \frac{dt}{d\tau} \ [°C/s],$$

(1)

where dt is the temperature variation during the period $d\tau$.

Several assumptions are taken into account in order to obtain the temperature-time function [4]:

- homogenous product;

- at any moment, the temperature is the same in the entire mass of the product;

- the temperature of the cooling medium is constant;

- there is no mass transfer between the product and the cooling medium.

The assumption that the sensible heat removed from the product equals the convective heat transfer from the product to the cooling medium leads to [4]:

$$m \cdot c \cdot dt = -S \cdot h \cdot (t - t_0) \cdot d\tau.$$

(2)

Eq. (2) finally leads to the temperature-time equation:

$$t = t_0 + (t_i - t_0) \cdot e^{-\frac{h \cdot S}{m \cdot c} \cdot \tau}. \tag{3}$$

The chilling duration is [4]:

$$\tau_r = \frac{m \cdot c}{h \cdot S} \cdot \ln \frac{t_i - t_0}{t_f - t_0}. \tag{4}$$

3. Chilling equipment

Food chilling is performed with mechanical refrigeration systems or with ice [4]. The temperature of the product should be lowered as quickly as possible through the critical warm zone (5–10°C), where maximum growth of microorganisms occurs [1, 3, 4].

Batch or continuous operation is possible when using mechanical refrigeration systems, while batch operation is used in the ice chilling systems.
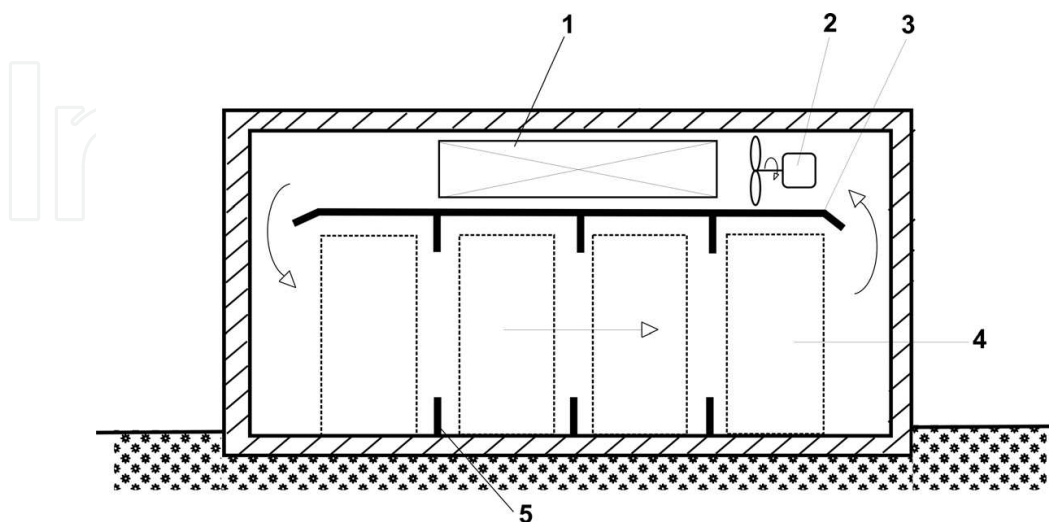
The chilling medium in mechanically cooled chillers may be air, water, or metal surfaces.

3.1. Air chilling

Air chillers use forced convection to circulate cold air at high speed (4 m/s); thus, the thickness of the boundary film is reduced, and the heat transfer rate is increased.
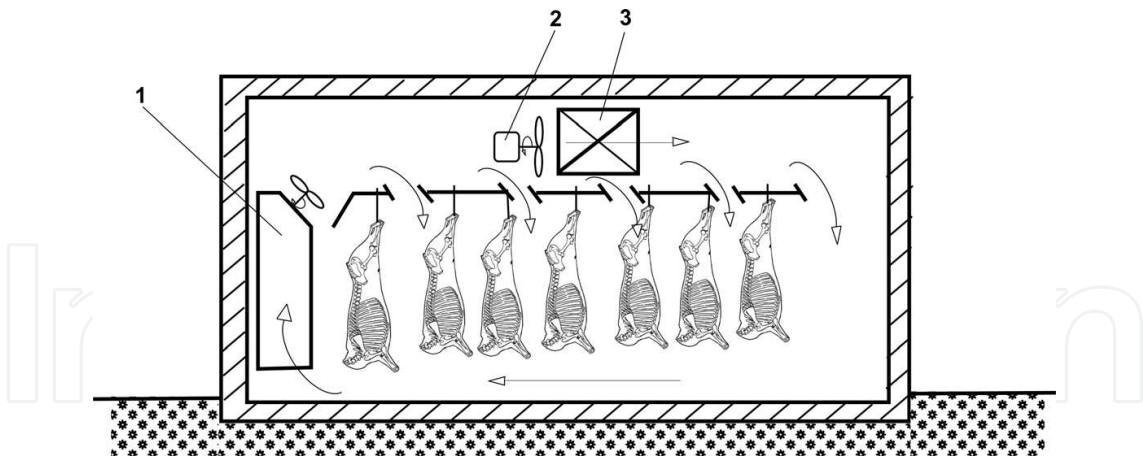
Air chilling of foods is performed in chilling tunnels or chilling rooms; usually, the chilling tunnels operate continuously, while the batch chilling is used for chilling rooms [4].

In a refrigeration tunnel, air circulates longitudinally, transversally, or vertically (**Figures 1** and **2**). Two-phase chilling can also be used in order to speed up the process and limit the evaporative weight losses [4]. **Figure 3** presents the schematic of the two-phase chilling tunnel. In the first
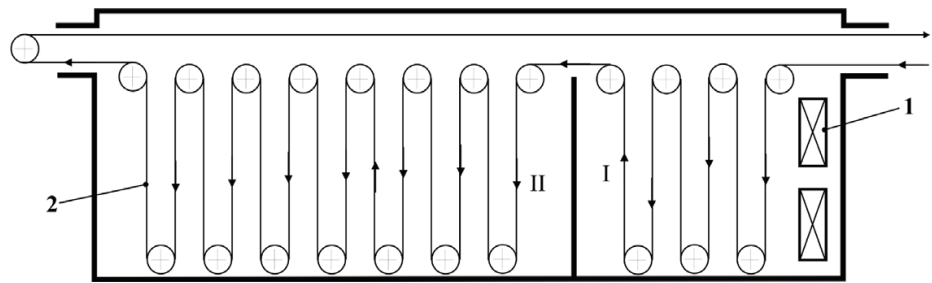

Figure 1. Air chilling tunnel, with longitudinal circulation of the air (vertical cross-section). 1, evaporator; 2, fan; 3, false ceiling; 4, product; 5, baffle.

Figure 2. Air chilling tunnel, with vertical circulation of the air (vertical cross-section). 1, 3, evaporators; 2, auxiliary fan.
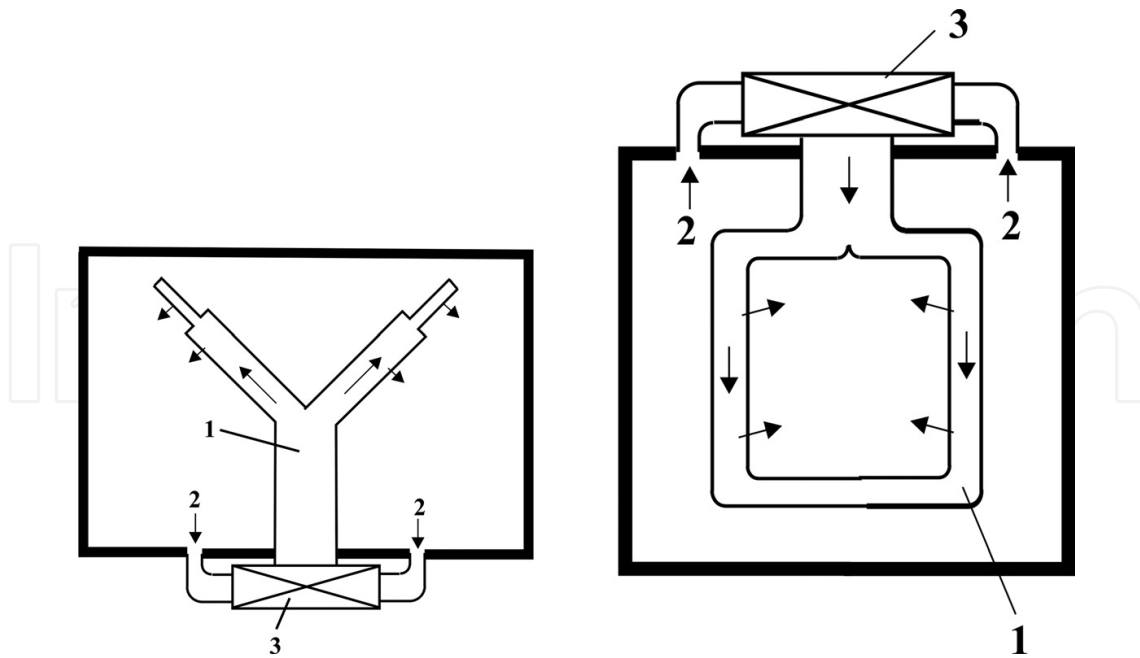

Figure 3. Two-phase chilling tunnel (horizontal cross-section). 1, evaporator; 2, conveyer; I, II, cooling sections.

chilling phase, the air temperature is around −10°C, and its speed is approximately 1 m/s; the products, hanged on the conveyer, travel through section (I) of the tunnel in about 4–5 h. The surface of the products is chilled rapidly in this first section. In the second section of the tunnel (II), air temperature is about 0°C, and its speed is 0.3 m/s; the duration of the chilling process is 10–15 h, until the product reaches a relatively uniform temperature in its entire mass [4]. This system allows the diminishing of the evaporative weight loss compared with the one-phase chilling systems because the surface of the product is quickly cooled in the first phase, and a lower temperature difference between the product and the cooling medium is achieved in the second phase.

Chilling rooms have a lower capacity than chilling tunnels; because of the lower air speed (0.3 m/s), the duration of the chilling process increases. **Figure 4** presents some examples of chilling rooms: the air discharge ducts are placed in the upper side of the room, while the air intake ports are placed in the lower part.

3.2. Chilling with liquid secondary agents

In this case, a chilled secondary agent is used in order to refrigerate the product; the product is sprayed with cold agent or is immersed into the chilling agent [1, 4, 5]. Due to the higher values of the convective coefficients, chilling with cold liquid agents requires less time than air chilling. The procedure is used for chilling poultry, fish, and some vegetable products [4, 5].
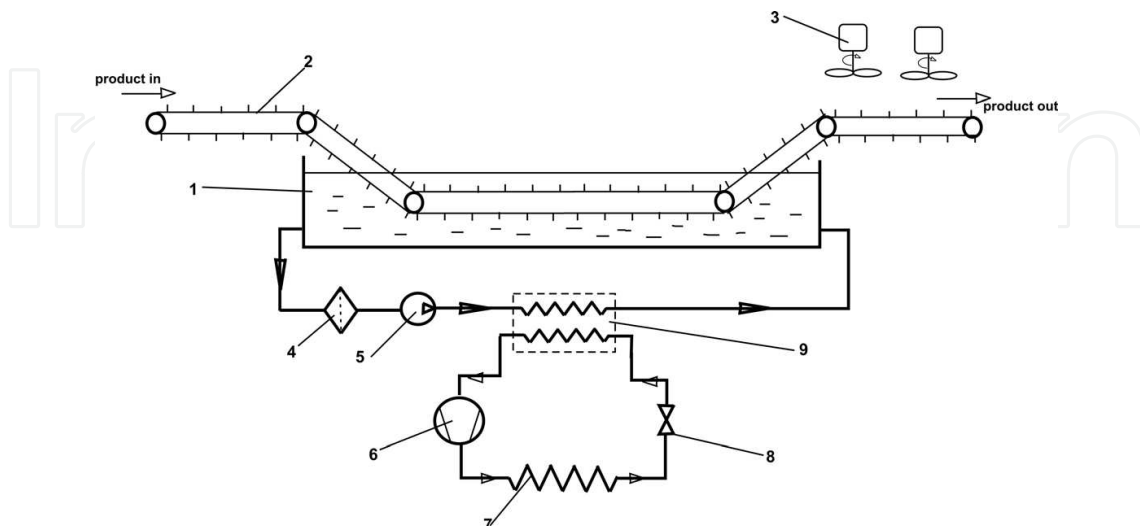
Figure 4. Chilling rooms. 1, discharge duct; 2, intake ports; 3, evaporator and fan.

Depending on the final temperature of the product and on the type of product, chilling may be achieved with water, salt water (brine), or slurry ice; ice or vapor compression refrigeration systems are used in order to cool the secondary agent [4].

Figure 5 presents the schematics of a device for the immersion chilling of poultry [1]; the carcasses are placed on the conveyor (2) and then immersed into the cold agent. The secondary agent is chilled in the heat exchanger (9) by a vapor compression refrigeration system.

Slurry ice is a phase-changing secondary agent, containing small ice crystals (typically 0.1–1 mm in diameter), suspended within a solution of water and a freezing point depressant. Some
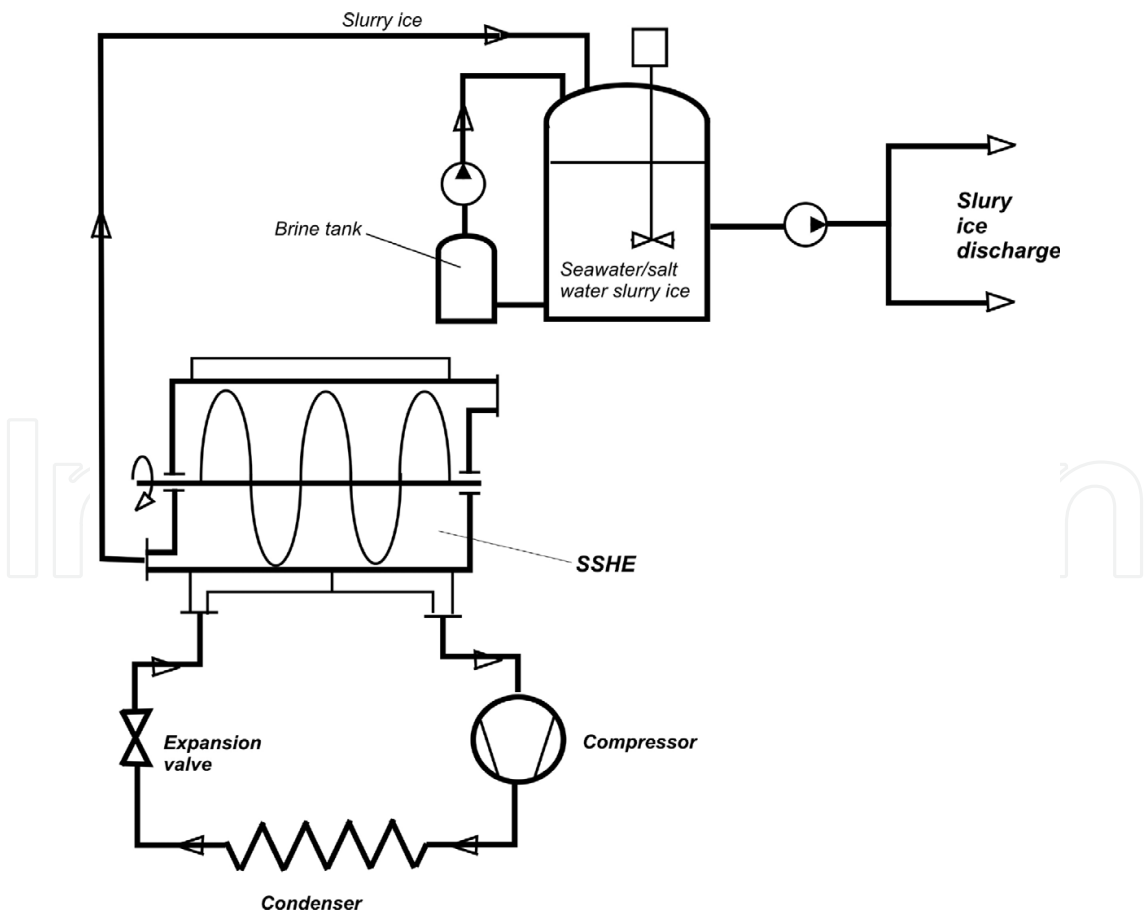
Figure 5. Immersion chilling of poultry. 1, immersion tank; 2, conveyor; 3, fan; 4, filter; 5, pump; 6, compressor; 7, condenser; 8, expansion valve; 9, heat exchanger.

commonly used compounds are salt (sodium chloride), ethylene glycol, propylene glycol, various alcohols (isobutyl, ethanol), and sugar (sucrose, glucose) [6]. This type of ice has many advantages in comparison with the traditional ice (flake ice, shell ice, crushed ice, etc.): it can be used in direct contact with the object to be chilled; due to the large contacting area, it has very good cooling performances; slurry ice can be pumped to the point of use (**Figure 6**), eliminating costly and maintenance intensive rakes, augers, and ice conveying systems [7]; operating at temperatures below the freezing point of water, ice slurry facilitates several efficiency improvements such as lowering the required temperature difference in heat exchangers due to the beneficial thermo-physical properties of ice slurry [6].
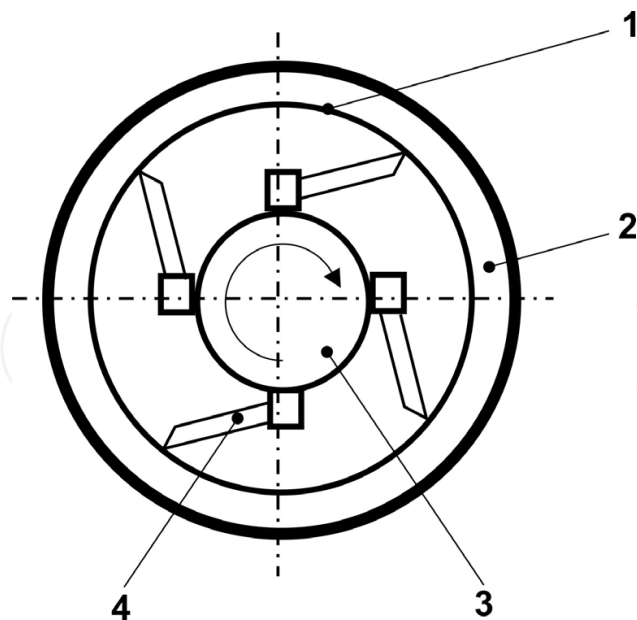
Slurry ice is produced in scrapped surface heat exchangers (SSHE); **Figure 7** presents the operating principle of the SSHE for slurry ice. The ice slurry generator consists of a cylindrical metal shell (1). The exterior surface is cooled by the evaporating refrigerant passing through the cooling jacket (2), while water freezes in contact with the cold inner surface of the shell. Spring-loaded rotating blades (4) scrap off the ice crystals formed on the inner cylindrical surface of the metallic shell.

3.3. Ice chilling

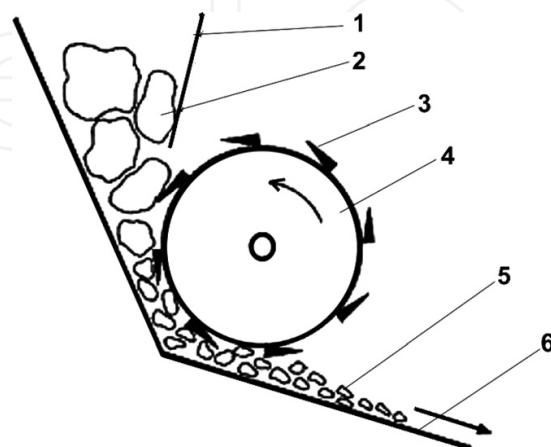This method is used for chilling fish and vegetables [1, 4].

Figure 6. Schematics of a slurry ice installation. SSHE, scrapped surface heat exchanger.

Figure 7. Schematic diagram of the ice slurry generator. 1, cylindrical metal shell; 2, cooling jacket; 3, rotating shaft; 4, blade.

Ice is often produced in the form of lumps or blocks, of various weights, from 10 to 200 kg. Alternatively, ice may be made in the form of smaller pieces (granular ice). Different types of granular ice exist (flake ice, tube ice, plate ice) [4].

In order to obtain ice blocks, the water to be frozen is filled into large metal molds, which are placed in a tank containing refrigerated brine, for up to 24 h. When the ice blocks are completely frozen, they are removed from the freezing tank and dipped into hot water. This melts the surface of the block so that it can be tipped out of its mold. The molds can then be refilled with water and returned to the freezing tanks. The large ice blocks may then be broken down into smaller pieces in an ice-crushing machine (**Figure 8**).

Figure 8. Ice-crushing machine. 1, infeed hopper; 2, large ice chunks; 3, blade; 4, rotating drum; 5, crushed ice; 6, discharge chute.

One of the most common types of granular ice is flake ice, which is obtained by freezing water onto the surface of a rotating, refrigerated drum (**Figure 9**). The water freezes into a 2–3-mm-thick layer of ice, which is then scraped off the drum as flakes of ice.
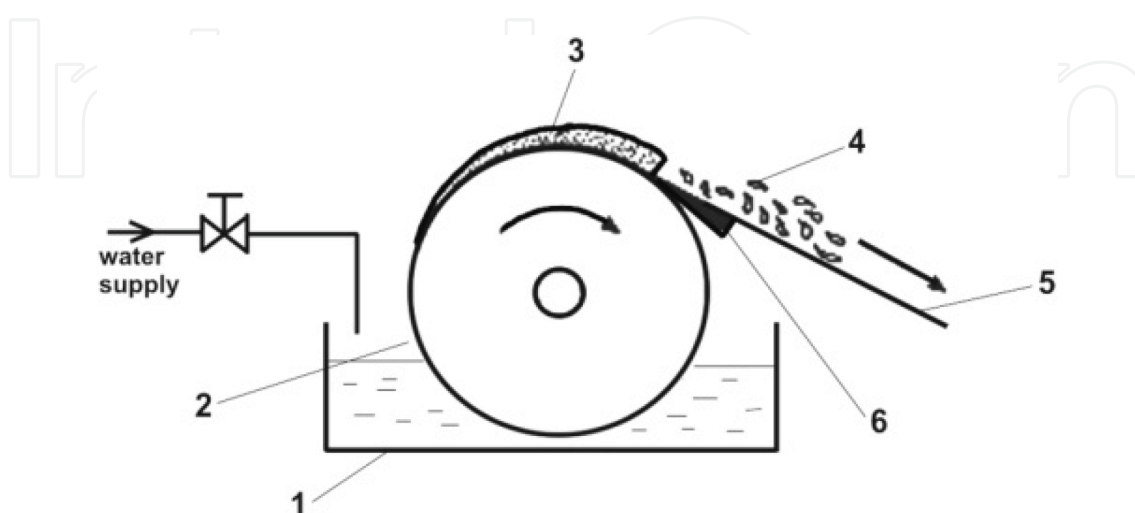
Storing fish in ice is largely used aboard fishing ships; apart from chilling the fish, ice removes heat from the surrounding structure of the box or storage compartments, absorbs the heat input through the structure from the warm air and sea outside, and removes the heat produced by the spoilage process in the fish themselves [8]. It is therefore essential that plenty of ice is properly distributed throughout the catch to ensure efficient cooling. Ideally, each fish should be in contact only with ice; in practice, there are alternating layers of ice and fish (**Figure 10**). The ice-to-fish ratio is comprised between 1/3 and 1/1; there should be at least 5 cm thick layers of ice (1, 3) between fish and the compartment walls [8]. In order to avoid the lower layers being damaged under the weight of the upper layers, fish must be placed on shelves, in order to keep the depth of the storage compartment (2) lower than 0.5 m [8].

Ice chilling is also used for vegetables and fruits [4]; the products are placed in wooden or cardboard crates, filled with ice. **Figure 11** presents the schematics of an ice-filling machine; the ice flakes flow into the machine hopper (2) through the chute (1) and are poured into the crates through the hopper (4).
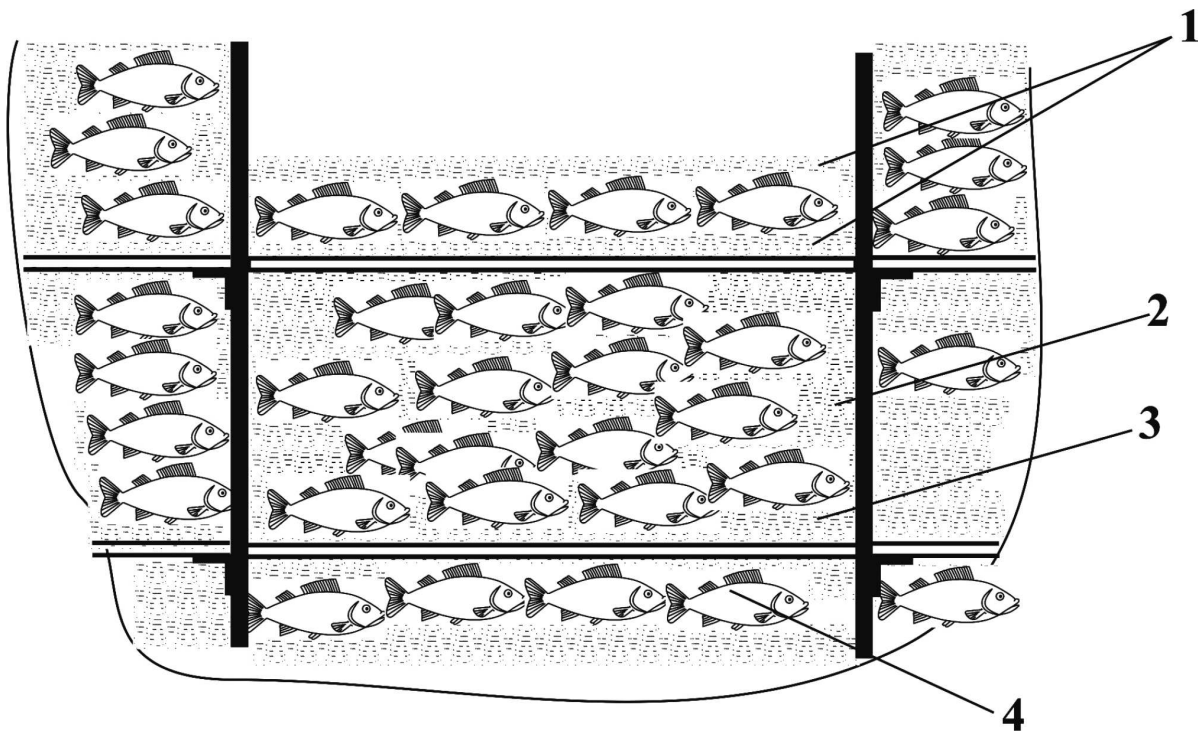
3.4. Chilling in tanks and heat exchangers

This chilling method is used for liquid food products (milk, cream, juices, beer, wine, etc.). Refrigerants or secondary cooling agents are used on the cold side of the chilling device, which is operated in batch or continuous mode [4].

In the batch operation mode, the product fed into the tank is cooled using an external cooling jacket or an internal cooling coil. **Figure 12** presents the schematics of a tank equipped with an external cooling jacket (2). The product is fed into the tank through the pipe (7); when the desired final temperature is reached, the product is purged from the tank through the discharge pipe (5).
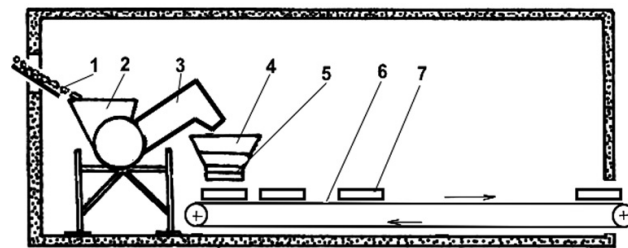

Figure 9. Production of ice flakes. 1, water tank; 2, rotating refrigerated drum; 3, ice layer; 4, ice flakes; 5, ice chute; 6, scrapper blade.

Figure 10. Fish chilling with ice. 1, 3, ice layers; 2, storage compartment; 4, fish.
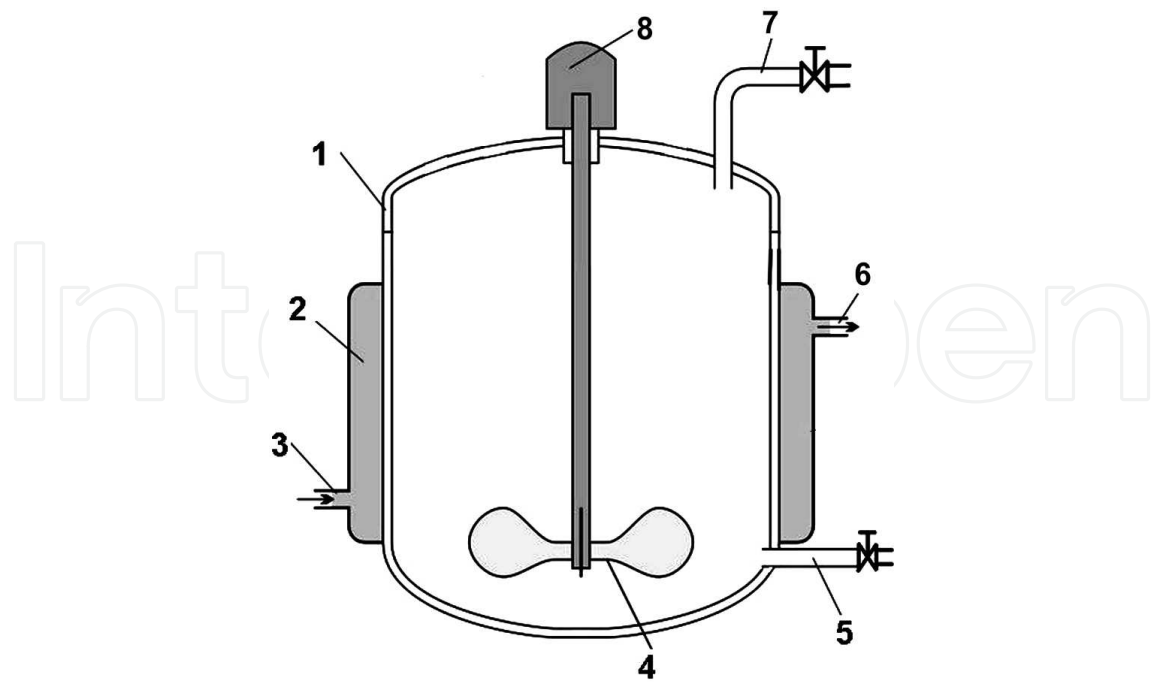
Figure 11. Ice-filling machine. 1, chute; 2, 4, hoppers; 3, flexible hose; 5, flap; 6, discharge conveyer; 7, crates.
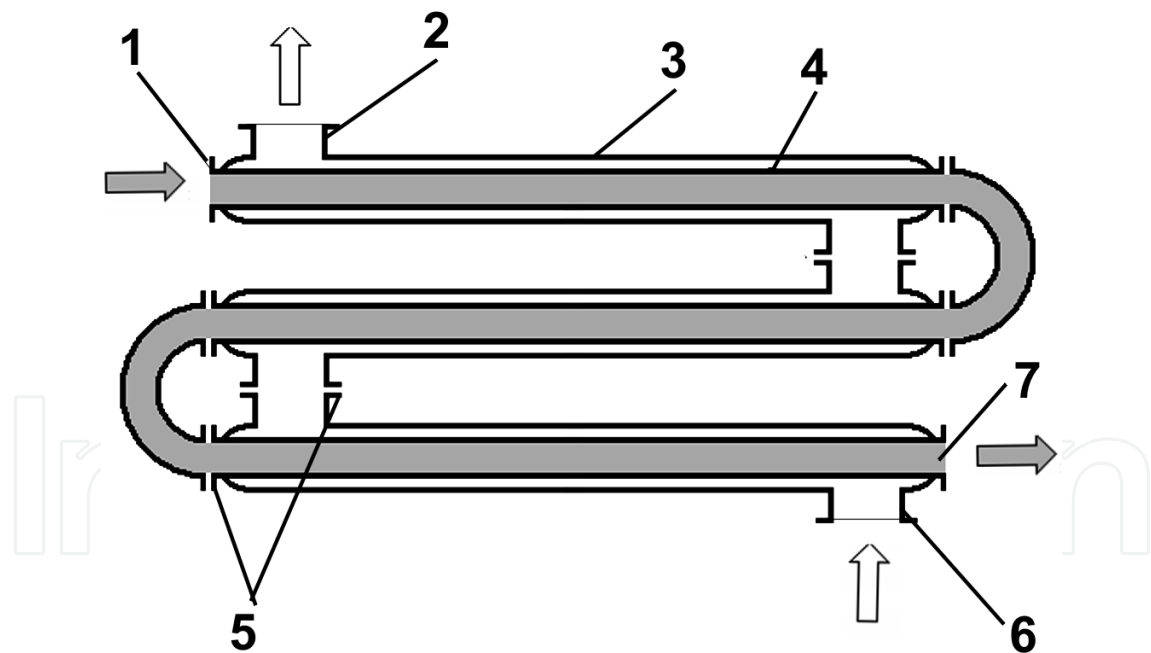
Heat exchangers are used in order to continuously chill the liquid products [3, 4]. **Figure 13** presents a double pipe heat exchanger; the cooling medium circulates through the shell (3), while the product circulates through the inner pipe (4). The exchanger contains several sections that are coupled through flanges; the number of sections depends on the final temperature and flow rate of the fluids [9].

3.5. Retail refrigeration cabinets

Retail refrigeration cabinets use cold air circulated through natural or forced convection. The cost of chill storage is high and, in order to reduce costs, large stores may have a centralized plant to circulate the refrigerant to all cabinets; the heat generated by the condensers of the refrigeration system may be used for in-store heating. Computer control of multiple cabinets detects excessive rises in temperature and warns of any requirement for emergency repairs or planned maintenance. Other energy-saving devices include night blinds or glass doors on the front of cabinets to trap cold air.

Figure 12. Chilling tank for batch operation. 1, tank; 2, cooling jacket; 3, coolant inlet; 4, stirrer.
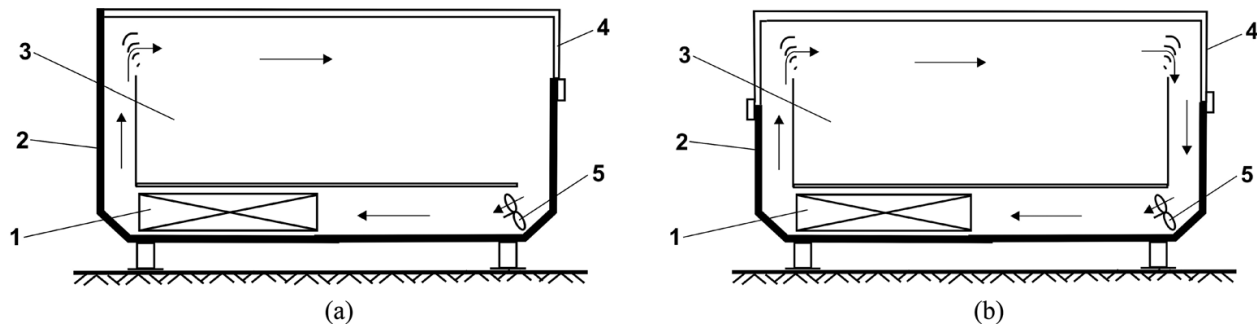

Figure 13. Double pipe heat exchanger. 1, product inlet connection; 2, refrigerant outlet connection; 3, outer shell; 4, inner pipe; 5, flanges; 6, refrigerant inlet connection; 7, product outlet connection.
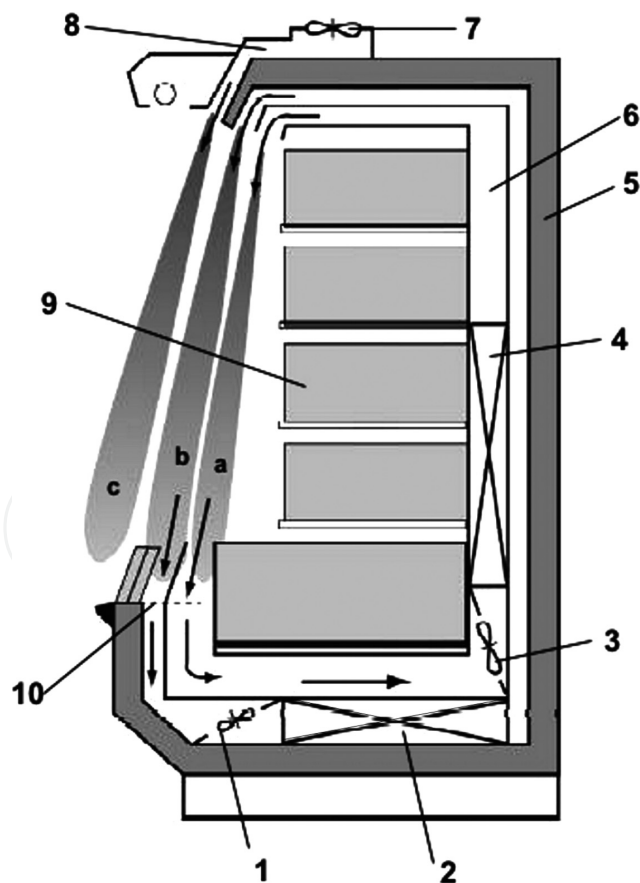
According to the cabinet geometry, the retail refrigeration cabinets are [10]:

- horizontal, single-deck units;
- vertical, multi-deck units.

Horizontal refrigeration cabinets (**Figure 14**) are open-top and are designed for self-service; the wall-site units (**Figure 14a**) allow shopping from one side, while the island type units (**Figure 14b**) are accessible from all sides [2, 10].

(a)   (b)

Figure 14. Horizontal refrigeration cabinets. 1, evaporator coil; 2, thermaly insulated case; 3, product loading space; 4, glass panels; 5, fan.

Figure 15. Vertical open front refrigeration cabinet. 1, 3, 7, fans; 2, 4, evaporator coils; 5, case; 6, 8, air channels; 9, products; 10, grills; a, b, c, air curtains.

Axial fans (6) are used to provide air flow over the evaporator coils (1), and grills placed at the upper side of the cabinet deflect the air current from one side of the cabinet to the other, over the stacked products. Due to cold air stratification, air infiltrations from the environment are relatively low; the heating load is due to the radiant heat transfer and conductive heat transfer through the insulated walls of the cabinet case [10].
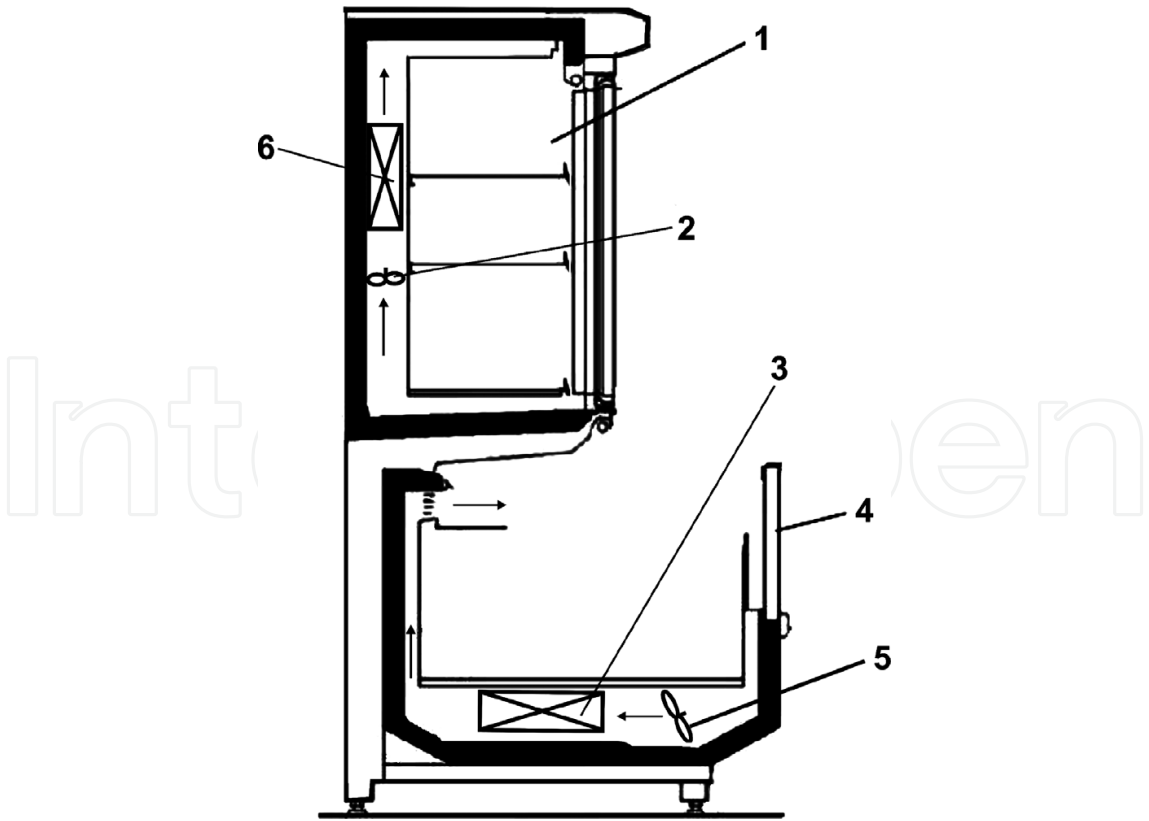
Vertical multi-deck units have an open front or are provided with a glass front door [2, 10]. The open front refrigeration cabinets (**Figure 15**) use air curtains (a, b, c) in order to prevent the infiltrations of warm air into the cabinet. The axial fans (1) and (3) circulate the cold air over the evaporator coils (2, 4) and produce the stream of air necessary for obtaining the inner air curtains; the outer air curtain (c) is generated by the axial fan (7). Grills are used in order to direct the air flow and obtain the air curtains.

The three air curtains form a very complex system, and the proper design imposes an in-depth understanding of the cabinet's fluid dynamics [2].
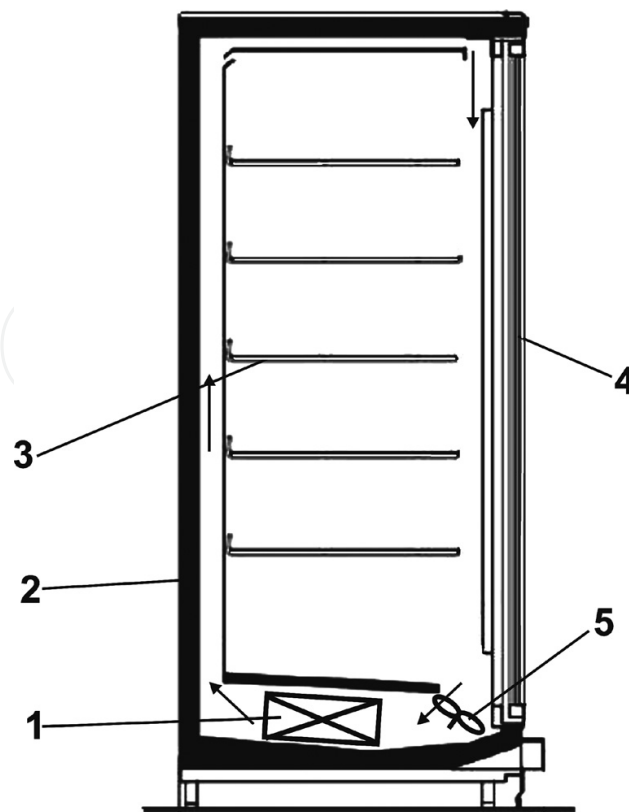
Some stores are equipped with combination cabinets (**Figure 16**), comprising an open front vertical cabinet and an open-top, horizontal cabinet [10].

The closed vertical refrigeration cabinets (**Figure 17**) use a glass door (4) in order to contain the products into the refrigerated space and prevent the infiltration of warm air [10].

Table 1 summarizes some characteristics of the retail display cabinets.

Figure 16. Combination cabinet. 1, vertical, open front, refrigeration cabinet; 2, 5, fans; 3, 6, evaporator coils; 4, horizontal, open type, refrigeration cabinet.

Figure 17. Vertical, closed, refrigeration cabinet. 1, evaporator; 2, case; 3, product shelves; 4, glass door; 5, fan.

Type	Refrigeration load [W/m]	Energy consumption [W/m]	Available volume [m³/m]
Horizontal, wall site	400–500	250–400	0.2–0.3
Horizontal, island	500–700	350–600	0.3–0.7
Vertical, closed	600–700	400–600	0.7–0.9
Vertical, open, three air curtains	1900–2200	1200–1900	0.7–0.8

Table 1. Characteristics of the retail display cabinets [10].

4. CFD modeling and simulation in a vertical refrigeration cabinet

Vertical refrigerating cabinets are widely used in supermarkets because the products have good storage conditions and are adequately presented to the consumers.

As mentioned above, the open type refrigerating cabinets use one or more air curtains in order to separate the cold interior from the warm surroundings.

The study of air curtains is necessary because these can be easily disrupted by air circulation in front of the cabinet or by the consumers taking foods from the shelves; the disturbing effect increases with the height of the cabinet. The aerodynamic non-homogeneity of the air curtain

increases when the number of "holes" increases, leading to the increase of the temperature inside the display case and of its power consumption; as a result, the products inside the cabinet are stored at temperatures higher that the recommended ones. Moreover, the infiltration of exterior humid air inside the case results in additional ice formation over the evaporator coils, thus reducing the heat transfer and the efficiency of the refrigeration system; therefore, the defrosting cycles become more frequent, further increasing the power consumption.

Some estimations show that 72–75% of the cooling load is used in order to counteract the effect of warm air infiltrations through the air curtain (**Figure 18**) and can reach even 90% if the operating conditions are not suitable [11]; 50% of the power consumption of a supermarket is due to the refrigeration and freezing cabinets.

CFD simulation was applied to a vertical display cabinet with four shelves, and in order to evaluate the temperature gradient, the following stages were taken into account: preprocessing —geometry set-up and design of the discretization scheme; processing—introduction of the boundary conditions and calculation; post-processing—visualization of the velocity and temperature fields.

4.1. CFD simulation and experimental tests

A refrigeration vertical cabinet with four shelves (**Figure 19**) was the basis of the simulation; the dimensions of the cabinet ($L \times W \times H$) are $1900 \times 796 \times 1911$ mm.

The axial fans (2) induce the airflow over the evaporator coil (3), placed at the bottom front part of the cabinet. A limited amount of air is fed into the unit, passing through the perforated plate behind the shelves (4), while the most significant amount of air flows through the horizontal
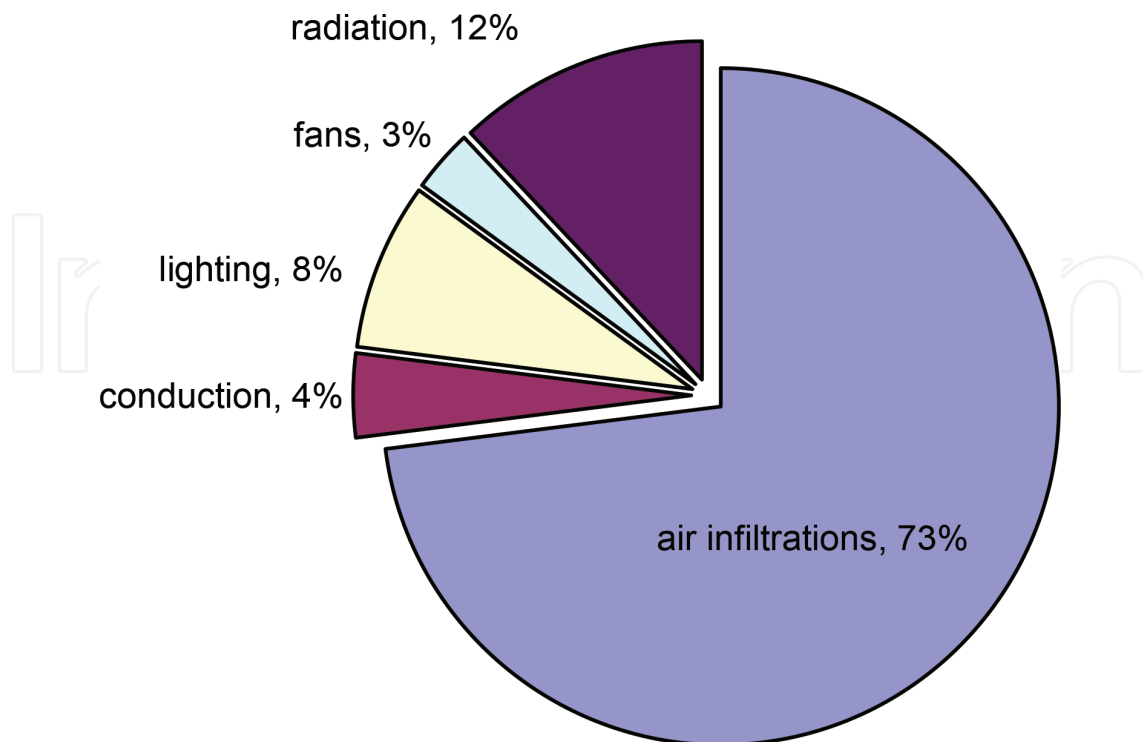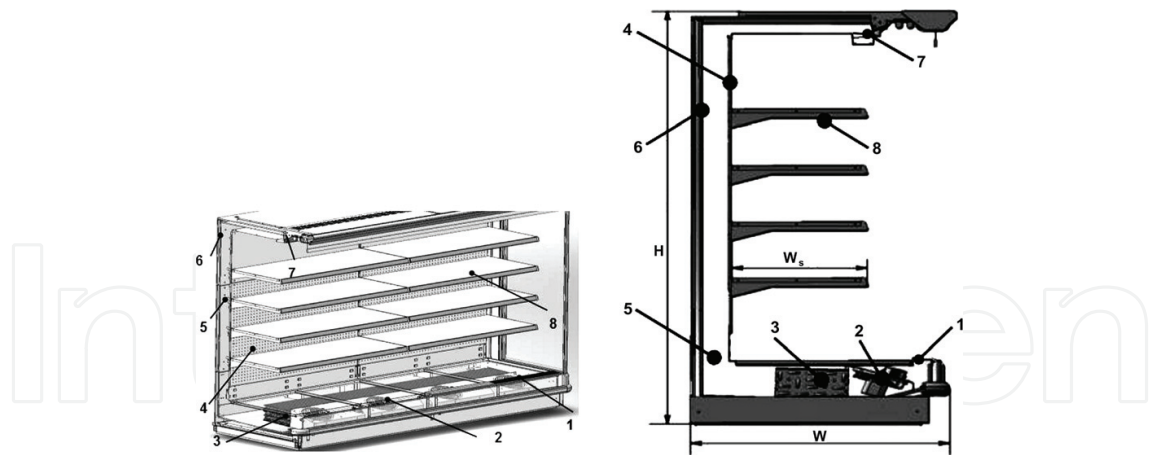

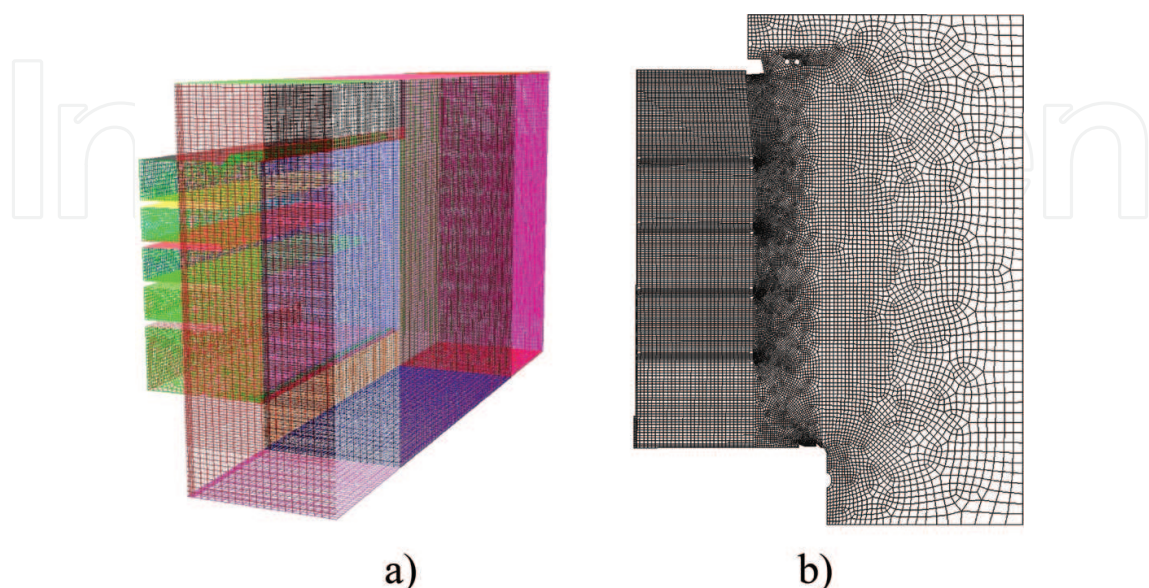**Figure 18.** Cooling load components.

Figure 19. Vertical display cabinet with four shelves. 1, base grill (GRA); 2, fans; 3, evaporator coil; 4, perforated plate; 5, air plenum; 6, thermal insulation; 7, horizontal grill (GPA); 8, shelves.
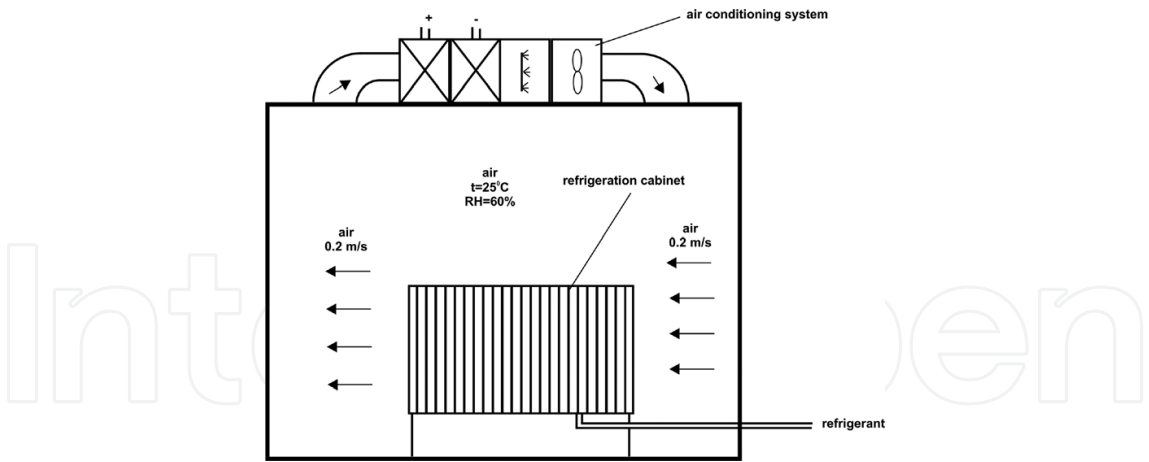
grill (7), thus creating the air curtain. The air curtain covers the front part of the shelves over their entire length; the air flows downward and is extracted through the base grill (1). The air curtain dimensions are as follows: thickness $B = 60$ mm; width of the shelves $W_s = 350$ mm.

The geometry of the air channels was used as a basis for producing the 3D model of the cabinet. The finite volumes discretization of the domain consisted of 1,585,690 nodes, being denser in the lower region of the cabinet (**Figure 20**).

In order to obtain the real boundary conditions, during the experimental tests, the refrigeration cabinet was placed inside a class 3 climatic chamber (according to EN-ISO 23953 and EN 441/4—**Figure 21**), which allowed the adjustment of different parameters of the ambient air (velocity, temperature, and humidity). During the tests, the air flow inside the chamber was parallel with the longitudinal axis of the cabinet, with a velocity of 0.2 m/s.

a)   b)

Figure 20. Structured discretization. a, view of the discretization domain; b, cross-section of the discretization domain.

Figure 21. Placement of the vertical refrigeration cabinet inside the climatic chamber.

Table 2 summarizes the transducers used in the experiments; the placement of the temperature, humidity, and velocity sensors in front of each shelf is shown in **Figure 22a**; temperature, humidity, and velocity sensors were also placed at the exit of the horizontal grill (GPA, **Figure 22b**); all the transducers were connected to a central data acquisition unit (**Figure 22c**). The sensors were placed in three vertical planes along the cabinet length: left, middle, and right (1, 2, 3, **Figure 23**).

Transducer type	Model	Purpose	Precision
Temperature	RTD, SEM 105 P	Ambient air temperature measurement	$\pm 0.1°C$
Temperature	TC with PTFE insulation	Temperature measurement inside the cabinet	$\pm 0.2°C$
Humidity	SEM 105H-3	Air humidity inside the cabinet and in the climatic test chamber	$\pm 0.3\%$
Velocity	Hot wire sensor, VelociCalc	Measurement of air velocity at the exit of GPA grill	± 0.015 m/s

Table 2. Summary of the transducers and their characteristics.

Figures 24 and **25** present the experimental results referring to the air velocity and temperature at the exit from the horizontal grill (GPA). The experimental data were then filtered using a C++ program; **Figures 26** and **27** show the filtered results.

Based on the charts presented in **Figures 26** and **27**, polynomial functions for the velocity and temperature variations were defined as:

a. velocity functions:

- left plane:

$$f(v_1, \tau) = (-1.4 \cdot 10^{16} \cdot v^{10} + 4.4 \cdot 10^{15} \cdot v^9 - 5.6 \cdot 10^{14} \cdot v^8 + 3.9 \cdot 10^{13} \cdot v^7 - 1.6 \cdot 10^{12} \cdot v^6 + 4.1 \cdot 10^{10} \cdot v^5 - 6.1 \cdot 10^8 v^4 + 4.8 \cdot 10^6 \cdot v^3 - 22484 \cdot v^2 + 162.5 \cdot v) + A_1 \cdot \sin(6.283 \cdot \tau/T_1); \tag{5}$$

- middle plane:

$$f(v_2, \tau) = (1.1 \cdot 10^{16} \cdot v^{10} - 4 \cdot 10^{15} \cdot v^9 + 5.6 \cdot 10^{14} \cdot v^8 - 4.3 \cdot 10^{13} \cdot v^7 + 1.9 \cdot 10^{12} \cdot v^6 -$$
$$5.2 \cdot 10^{10} \cdot v^5 + 7.7 \cdot 10^8 v^4 - 5.8 \cdot 10^6 \cdot v^3 + 18574 \cdot v^2 + 4.2 \cdot v) + A_2 \cdot \sin(6.283 \cdot \tau / T_2);$$

(6)

- right plane:

$$f(v_3, \tau) = (-2.1 \cdot 10^{15} \cdot v^{10} + 6.9 \cdot 10^{14} \cdot v^9 - 9.5 \cdot 10^{13} \cdot v^8 + 7 \cdot 10^{12} \cdot v^7 - 3 \cdot 10^{11} \cdot v^6 + 7.5 \cdot 10^9 \cdot$$
$$v^5 - 1 \cdot 10^8 v^4 + 8.7 \cdot 10^5 \cdot v^3 - 11436 \cdot v^2 + 167.91 \cdot v) + A_3 \cdot \sin(6.283 \cdot t / T_3).$$

(7)

b.   temperature functions:

- left plane:

$$g(t, \tau) = t_{1med} + A_{11} \cdot \sin\left(\frac{6.283 \cdot \tau}{T_{11}}\right);$$

(8)

- middle plane:

$$g(t, \tau) = t_{2med} + A_{22} \cdot \sin\left(\frac{6.283 \cdot \tau}{T_{22}}\right);$$

(9)

- right plane:

$$g(t, \tau) = t_{3med} + A_{22} \cdot \sin\left(\frac{6.283 \cdot \tau}{T_{33}}\right).$$

(10)

The above functions were introduced as user defined functions (UDF) into the numeric model.

4.2. The numeric model

The general equation for the incompressible flow of a fluid for a dependent variable Φ ($\Phi = 1$ for the continuity equation; $\Phi = v$ for the momentum equation; $\Phi = t$ for the energy equation) is [12]:
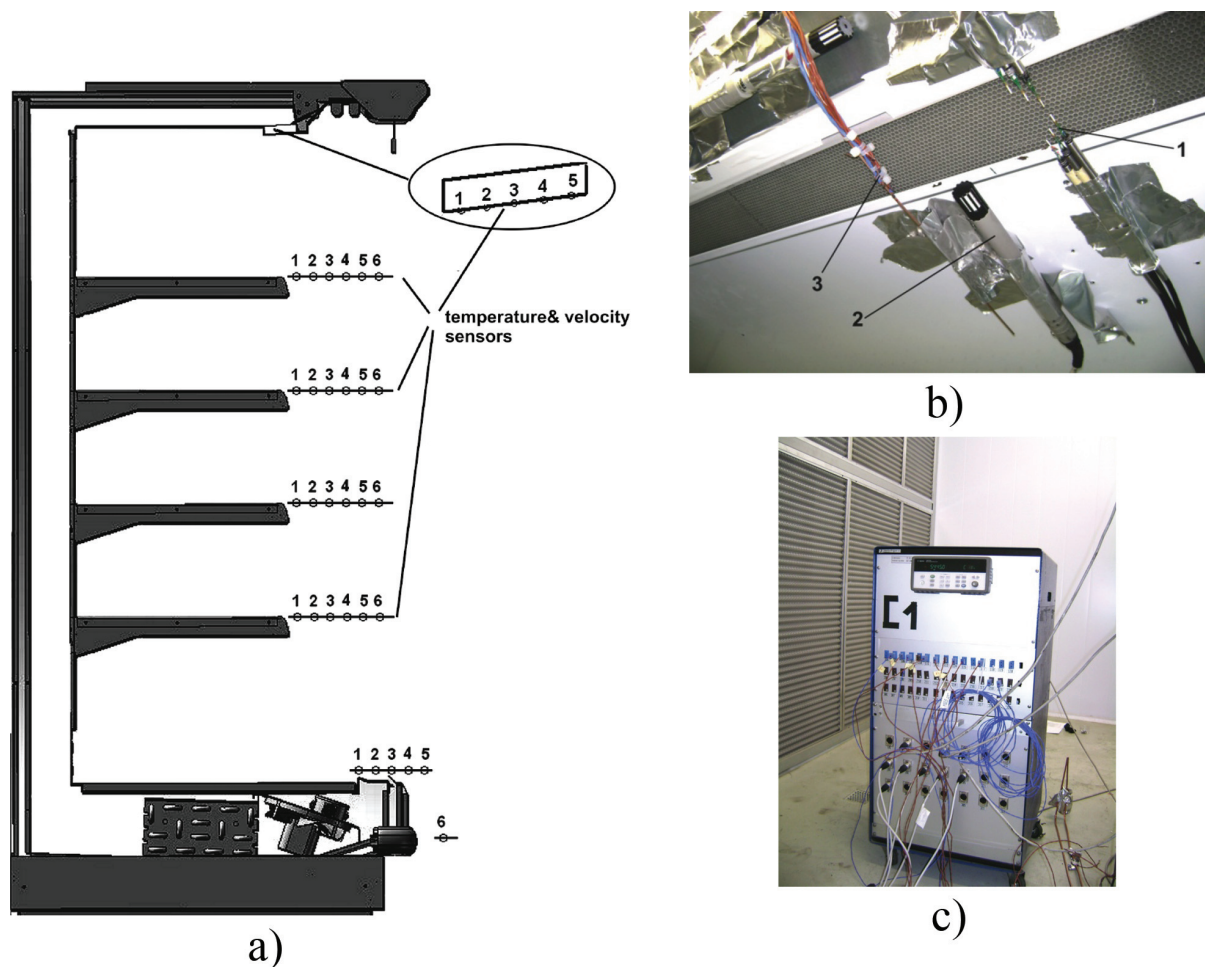
$$\frac{\partial}{\partial x_i}\left(\rho v \phi - \Gamma_\phi \frac{\partial \phi}{\partial x_i}\right) = S_\phi.$$

(11)

The model is based on the following assumptions:

- air is considered a perfect gas;

- the latent heat of condensation for the humidity in the air curtain is neglected;

- the air curtain is considered as a jet;

- air velocity and temperature at the horizontal grill are modeled as polynomial functions;

- the effect of air flowing through the holes of the perforated plate behind the shelves is neglected.

The model is based on two equations (one for the turbulent kinetic energy and the other one for the dissipation rate of the turbulent kinetic energy), using the SIMPLE algorithm. The

Figure 22. Placement of the sensors and the central data acquisition unit. a, placement of the temperature, humidity, and velocity sensors inside the cabinet; b, placement of the temperature, humidity, and velocity sensors at GPA grill; c, view of the central data acquisition unit.

calculation is an iterative process, using the pressure-velocity coupling algorithm, in which the momentum and continuity equations, based on pressure, is solved simultaneously, and the terms referring to the pressure gradient and mass flow rate are discretized implicitly.

4.3. Boundary conditions

The boundary conditions were imposed by the pre-processing program Gambit and completed with functions and values in the Fluent CFD simulation program [12]. The boundary conditions also took into account the conditions inside the climatic chamber ($t_{env} = 25°C$, $\Phi_{env} = 60\%$, $v_{air} = 0.2$ m/s, according to EN-ISO 23953); as there are different boundary conditions for the horizontal grill (GPA) and base grill (GRA), these are presented separately.
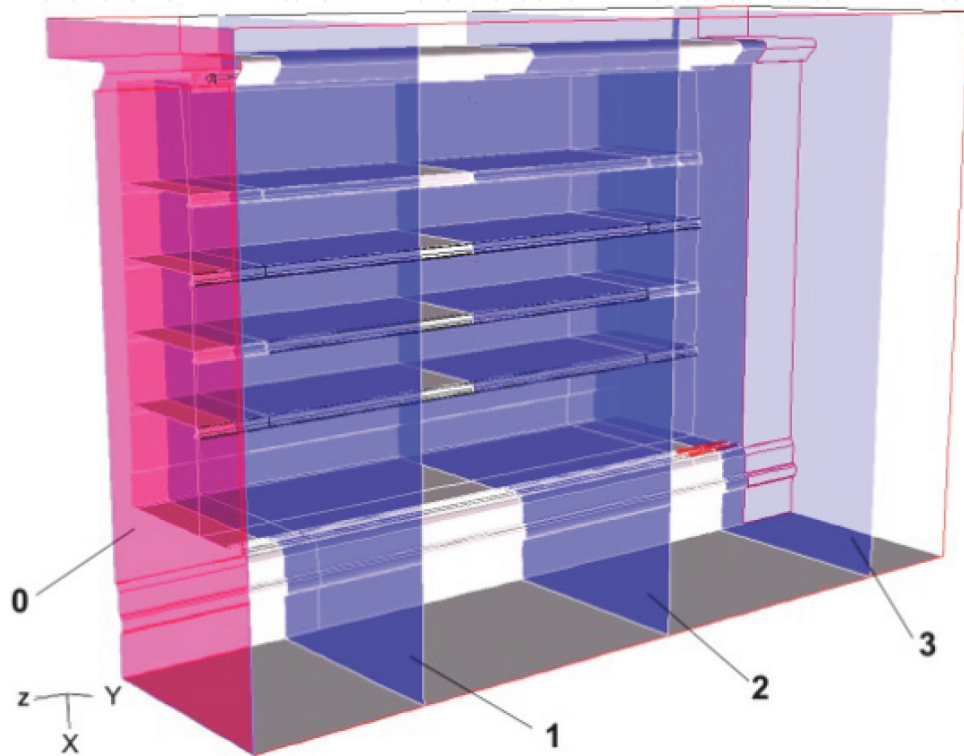
4.3.1. Boundary conditions for GPA

The velocity and temperature functions, for the three vertical planes considered (left, middle, and right), were the ones presented above. The air turbulence was specified using the turbulence intensity [12]:
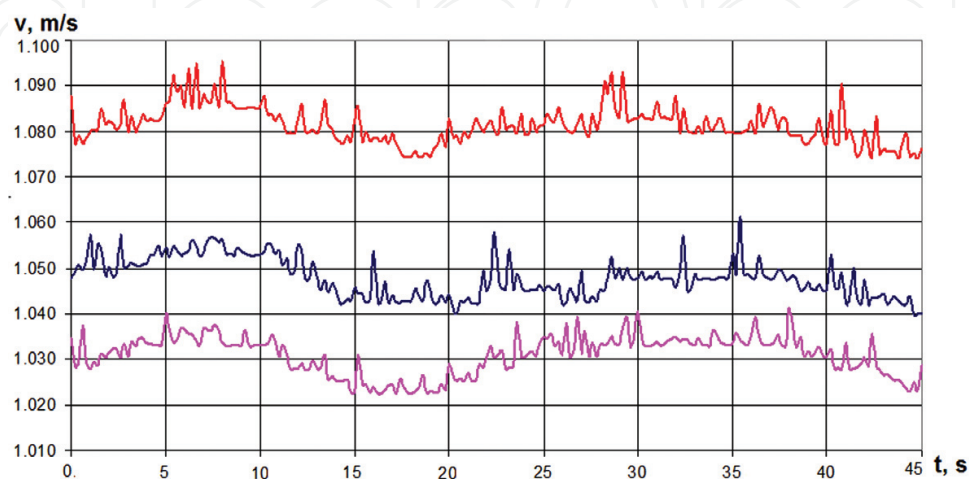
$$I_t = 0.16 \cdot \text{Re}_{Dh}^{-0.125} \cdot 100. \tag{12}$$

Turbulence intensity at GPA exit had the following values: $I_t = 2.66$ (left plane); $I_t = 1.83$ (middle plane); $I_t = 2.16$ (right plane).

A boundary condition was also imposed for the lateral plane (0, **Figure 23**); here, air velocity was constant over the entire section (0.2 m/s), the flow was laminar, and air temperature was 25°C.

Figure 23. Measuring planes. 0, lateral plane, with air entering at 0.2 m/s; 1, left plane; 2, middle plane; 3, right plane.
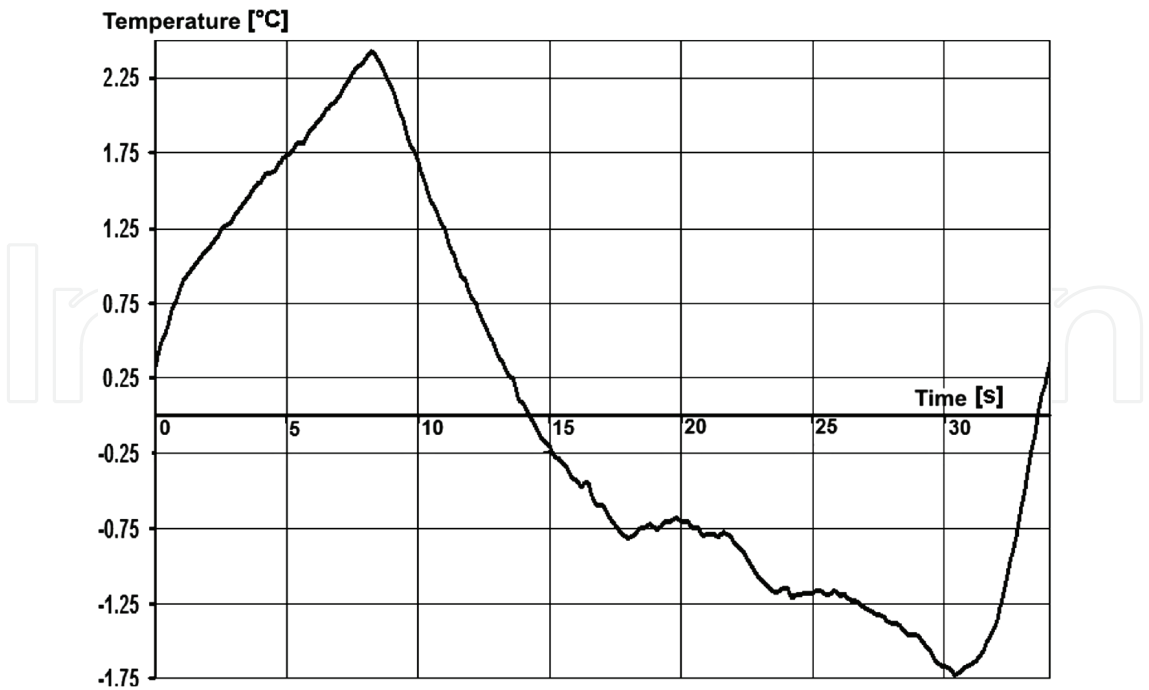

Figure 24. Air velocity at the GPA level.

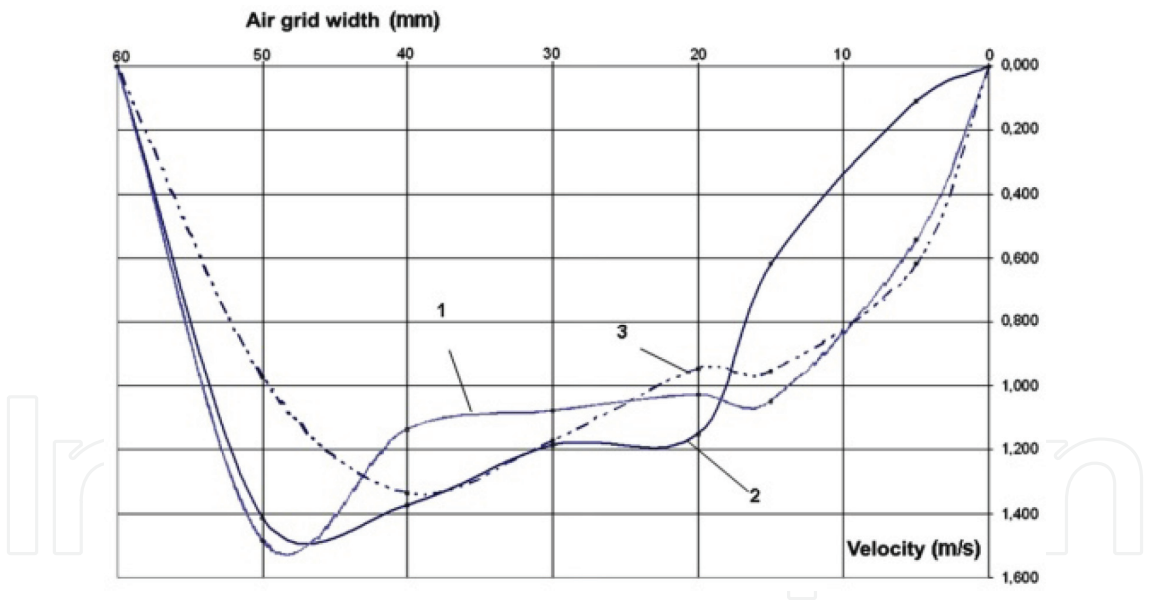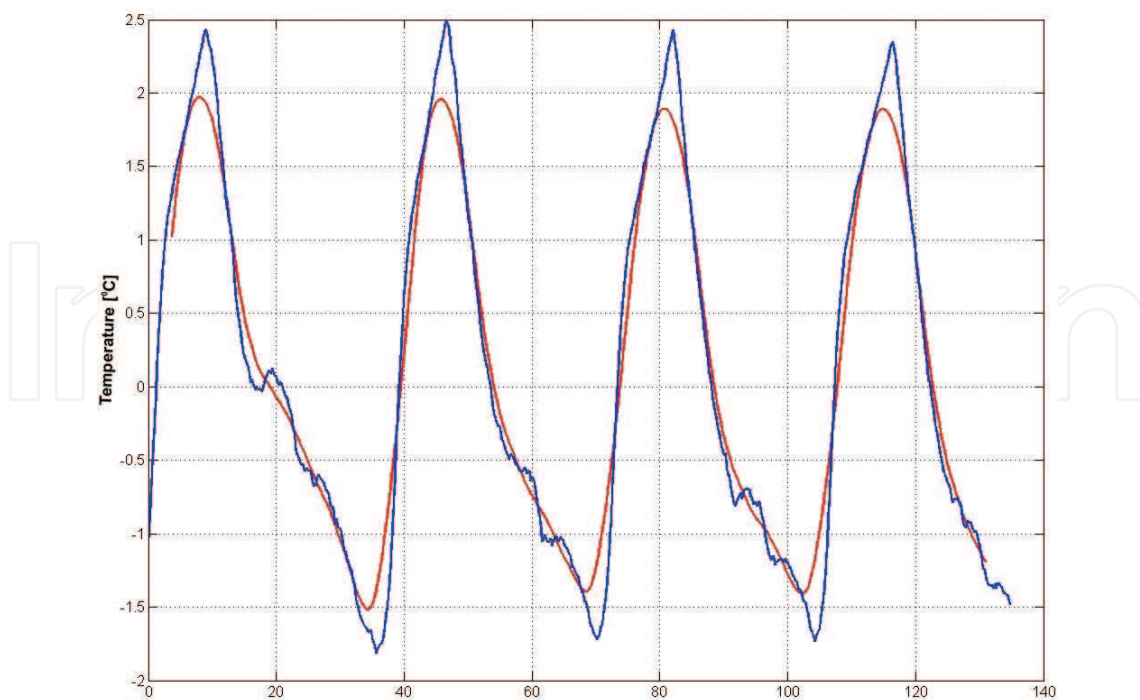**Figure 25.** Air temperature at the GPA level.

Figure 26. Air velocity profiles, after filtering, for the three vertical planes.

4.3.2. Boundary conditions for GRA

The boundary conditions for the base grill take into account the average experimental values: over the entire length of the grill, air velocity is 1.7 m/s, and air temperature is +9.2°C. The air turbulence parameters were defined as above.

Figure 27. Air temperature profiles, after filtering, for the three vertical planes.

4.3.3. Boundary conditions for heat flow rate

The boundary conditions for the heat flow rate take into account the conductive heat transfer through the cabinet walls and the heat generated by the illumination system of the display case.

The conductive heat transfer was defined using Fourier's law; the overall heat transfer coefficient was calculated based on the thermal conductivity of each individual layer of the respective wall. The conductive heat transfer rates were as follows: 6 W/m^2 for the ceiling of the cabinet; 7 W/m^2 for the bottom of the cabinet; and 7.63 W/m^2 for the side walls.

Fluorescent lamps, type OSRAM L58W20, were used for the illumination of the appliance; the corresponding heat flow rate was 10 W/m^2.

4.3.4. Boundary conditions for the walls

The cabinet walls were modeled only in the wall-air contact areas. The average temperatures were obtained experimentally, as follows: evaporator fins—0.95°C; interior walls +7°C; shelves +5°C.

4.3.5. Product thermal load

According to the EN-ISO 23953 standard, the load is simulated using a gel-type substance (tylose), with thermal properties similar to the ones of beef meat. However, in the present simulation, there was no product load inside the cabinet.

4.4. Processing

In the processing stage, the time step was set at 0.2 s, the number of steps was 1800, and the maximum number of iterations for one step was 10.

The simulation was performed on a Pentium IV, DualCore 6400, 2.4 GHz system with 4 GB RAM; for 6 min of simulation and a total number of 18,000 iterations, the computing time was approximately 12 h.

In order to prevent the equation coefficients from changing too quickly, the change in dependent variables from one iteration to another was slowed by "relaxing" them. Thus, the linear relaxation method was used for the control of the CFD simulation in order to maintain its stability; **Table 3** presents the values of the relaxation factors for the different physical parameters.

Property	Variable	Relaxation factor, α
Pressure	p	0.3
Density	ρ	0.5
Lift force	F	0.5
Momentum	v_i	0.8
Turbulent kinetic energy	k	0.6
Dissipation rate of the turbulent kinetic energy	ε	0.6
Turbulent viscosity	μ_t	0.8
Energy	E	0.7

Table 3. Linear relaxation factors.

In this CFD simulation, the convergence criterion was selected so that the residues remained lower than 10^{-6}.
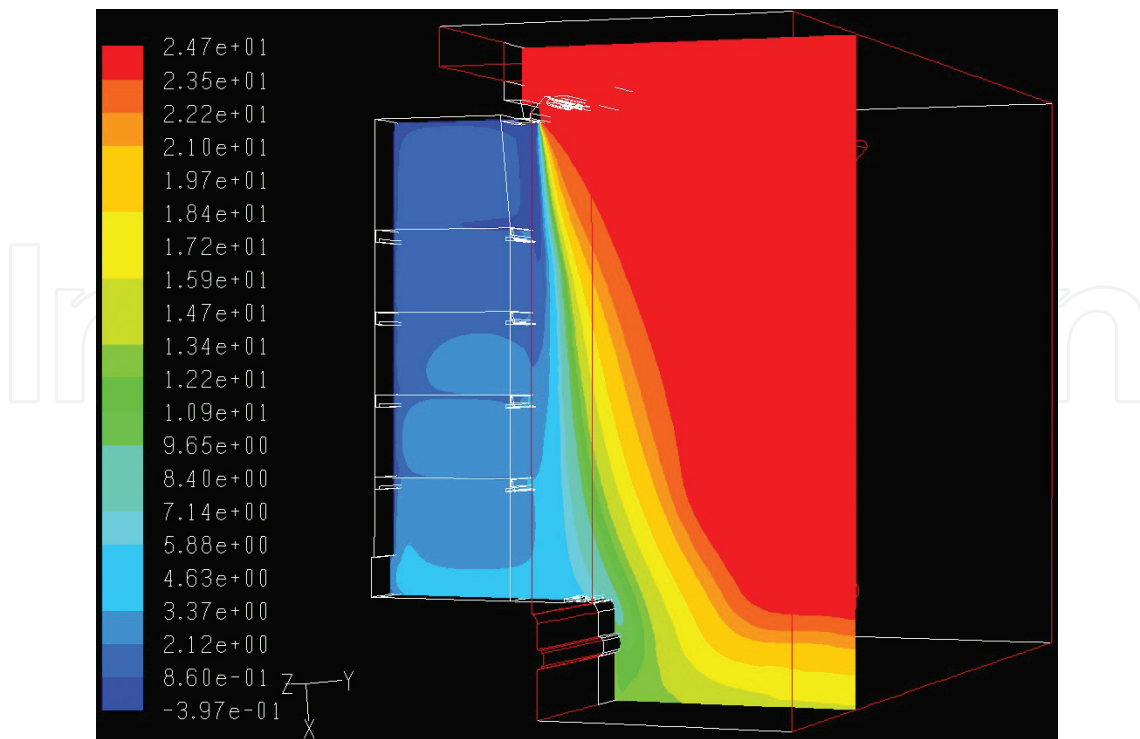
4.5. Post-processing

Post-processing is the final stage of the CFD simulation, aiming to display the temperature and velocity fields, as well as the streamlines in the simulation domain. This stage is useful in the intermediate phases of the simulation, allowing its calibration based on the experimental data; at the end of the simulation, the final temperature and velocity fields and the streamlines are presented in a graphical form.
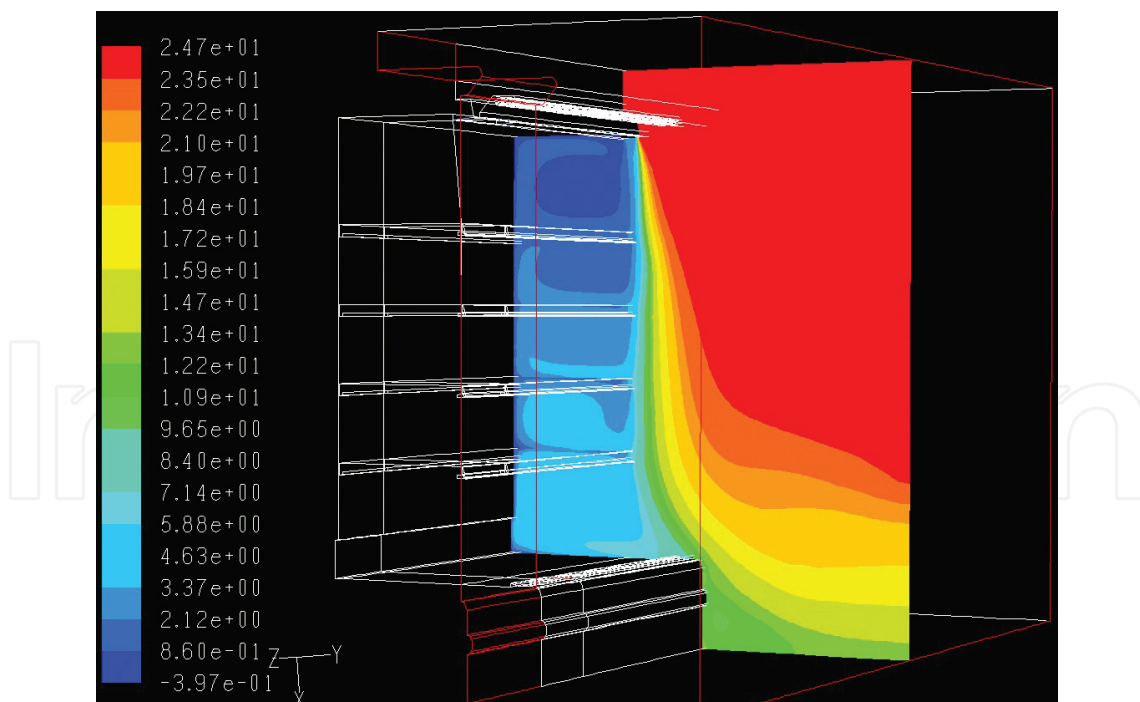
Figures 28–30 present the temperature fields in the three vertical planes taken into account (see **Figure 23**); the results show that, for the lower shelves, the temperature is with at least 4°C higher than the one required (5°C, according to ISO 23954-2:2005), which means that this area is not adequate for the storage of refrigerated goods.

Figure 31 presents the velocity field profile in the middle plane, at the exit of the horizontal grill (GPA).

Figure 32 presents the velocity field in the vertical right plane and also in the horizontal plane, in the vicinity of the base air grill (GRA). In the horizontal plane, air velocity was comprised

Figure 28. Temperature field in the left plane of the cabinet, at the end of the 6 min simulation [°C].

Figure 29. Temperature field in the middle plane of the cabinet, at the end of the 6 min simulation [°C].

between 0.4 and 0.6 m/s; these values were significantly lower than the average value of 1.7 m/s, which was considered as a boundary condition for GRA, showing the non-uniformity of the air curtain in this area.
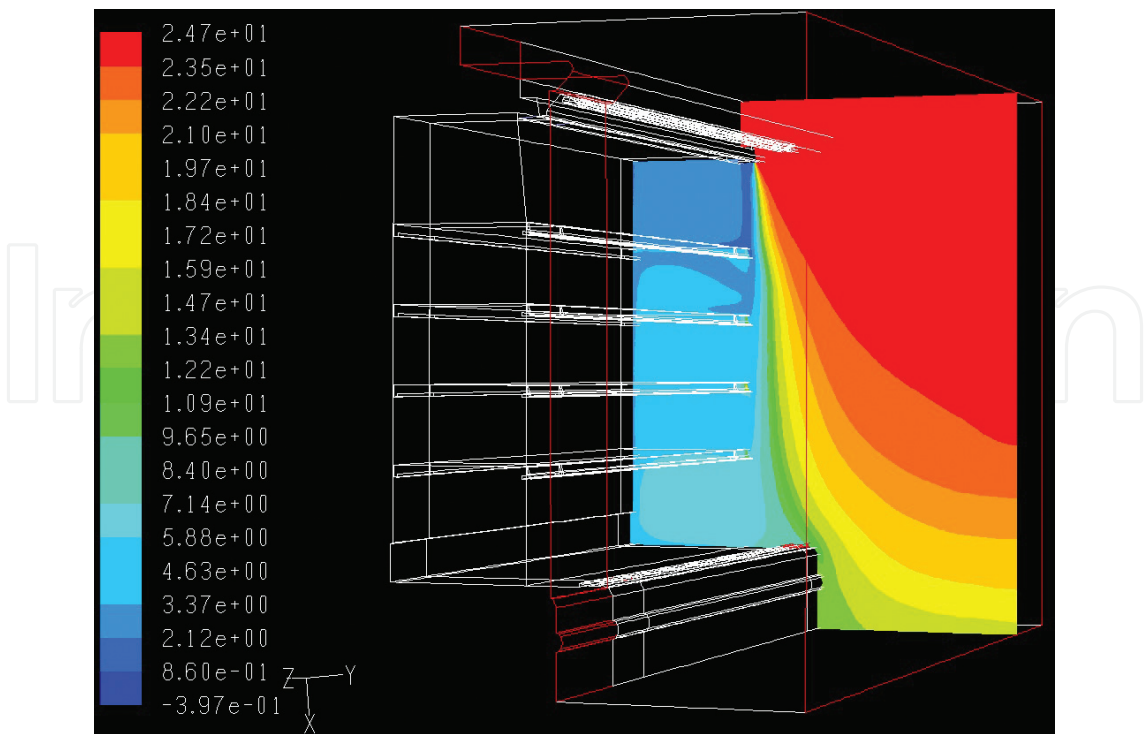
Figure 30. Temperature field in the right plane of the cabinet, at the end of the 6 min simulation [°C].

The streamlines presented in **Figure 33** complete the picture of the air curtain in terms of air velocity, while **Figures 34** and **35** display the streamlines in terms of air temperature; the results can be summarized as follows:
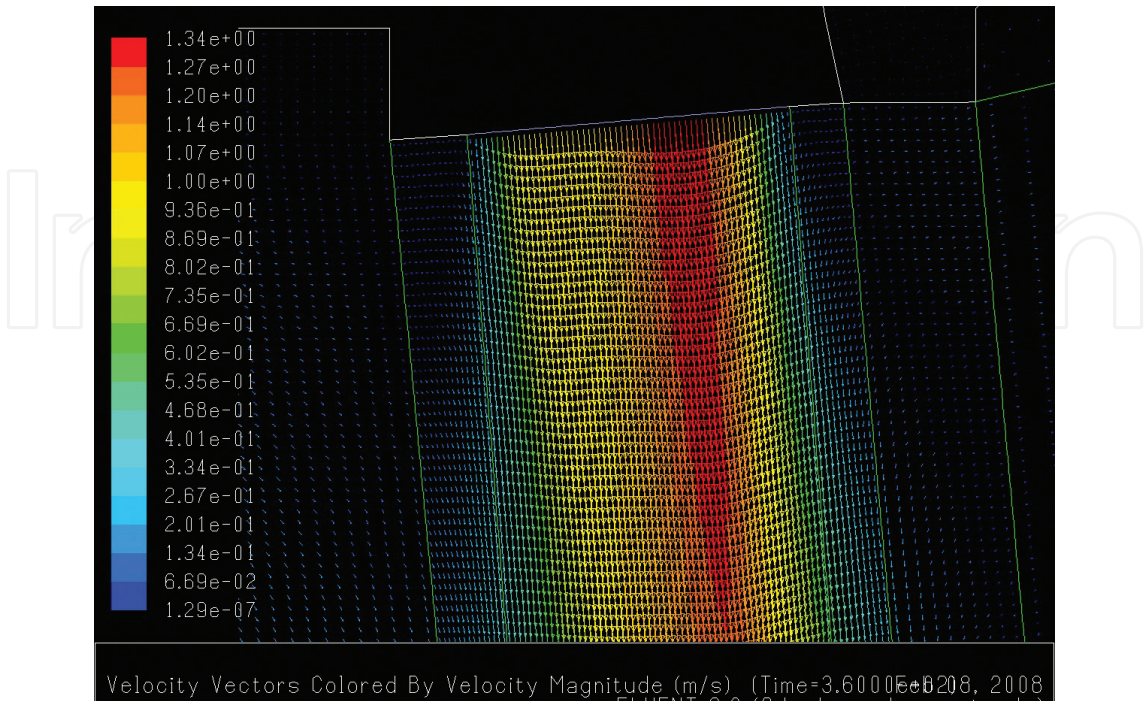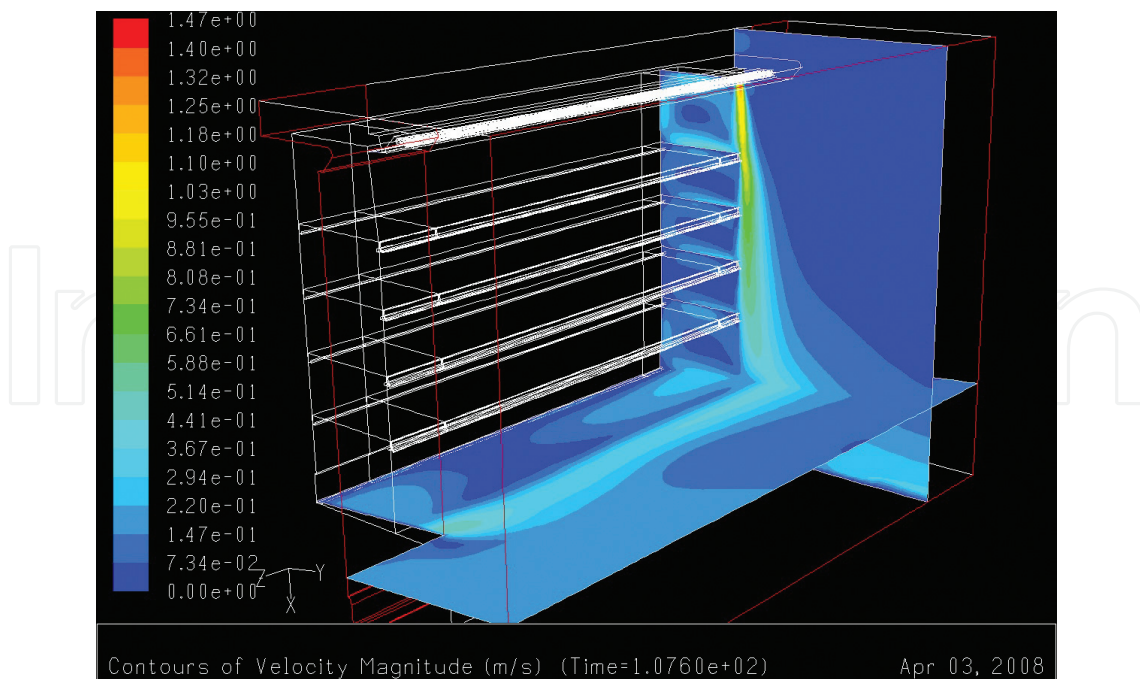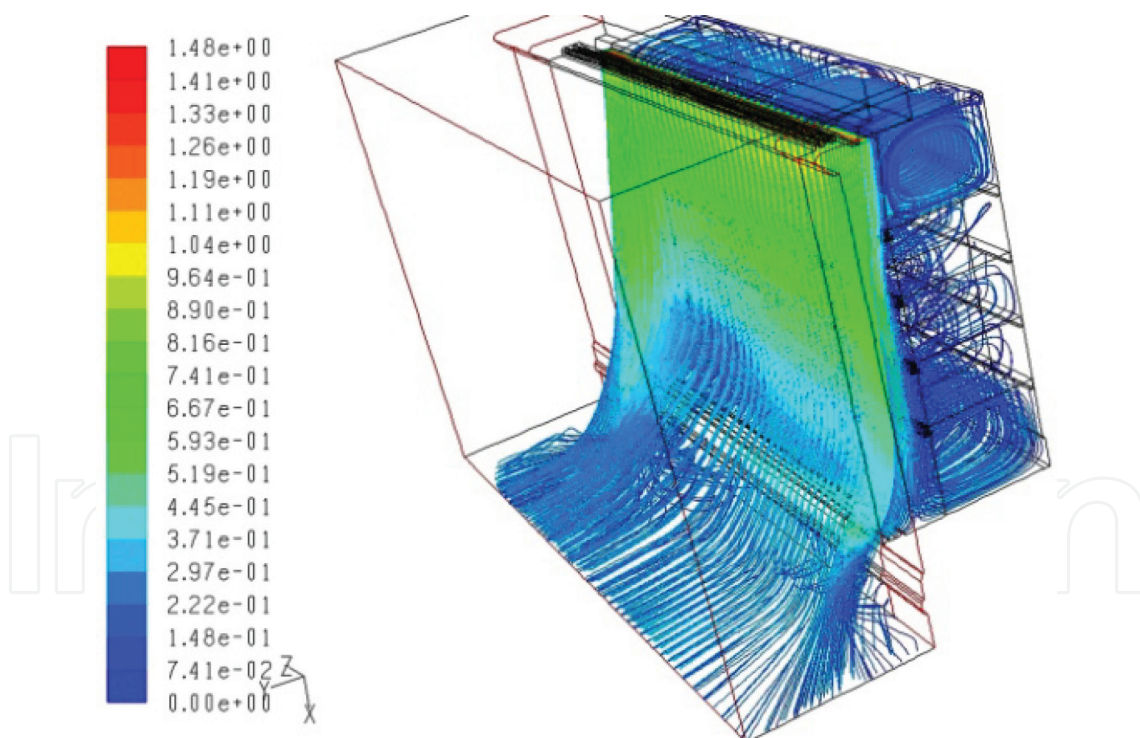

Figure 31. Velocity field profile at GPA, in the middle plane, at the end of the simulation.
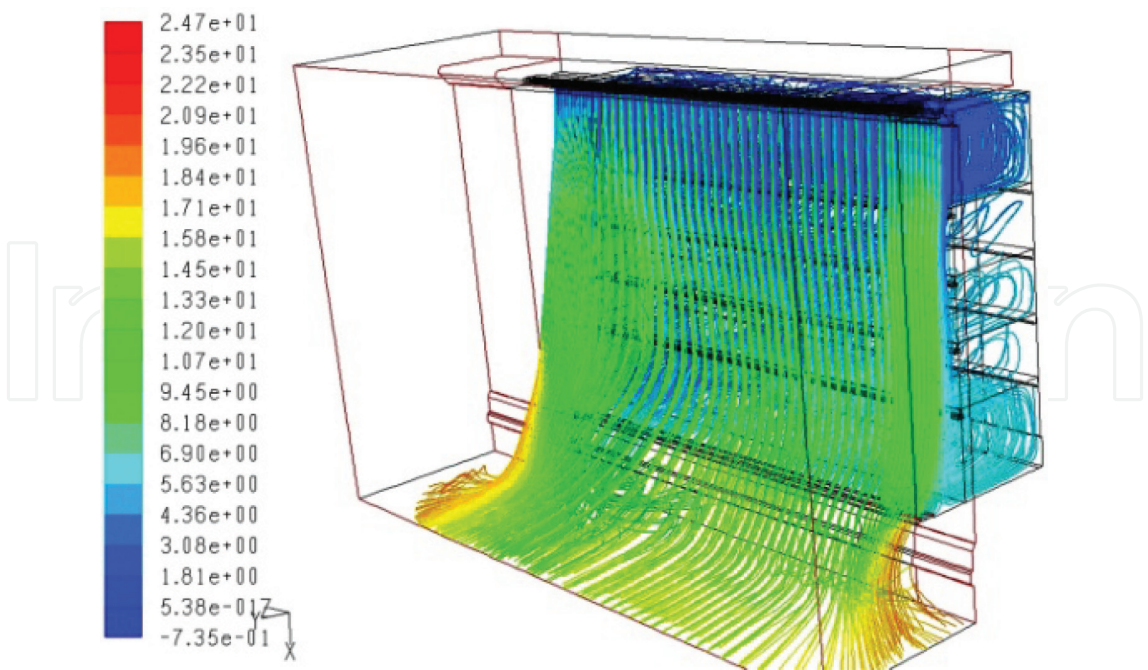
Figure 32. Velocity field profile in the vicinity of GRA and in the vertical right plane.

Figure 33. Streamlines for air velocity [m/s].

- the turbulence and temperature are higher at the back of the cabinet;

- the infiltration rate through the air curtain is higher in the lower part of the cabinet, through the left and right planes;

- the temperature difference between the upper and lower shelves is 6°C.

Figure 34. Streamlines for air temperature, front view [°C].

Figure 35. Streamlines for air temperature, rear view [°C].

5. Conclusions

Refrigeration slows down the chemical and biological processes in foods, such as the accompanying deterioration and the loss of quality, extending the shelf life of the products.

Food chilling is performed with mechanical refrigeration systems or with ice; the temperature of the product is lowered to 0–8°C, depending on the type of food. The chilling medium in mechanically cooled chillers may be air, water, or metal surfaces; batch or continuous operation is possible when using mechanical refrigeration systems, while the batch operation is used in the ice chilling systems.

Retail refrigeration cabinets use cold air, circulated through natural or forced convection. The open front refrigeration cabinets use air curtains in order to prevent the infiltrations of warm air into the cabinet; the proper design of the air curtains imposes an in-depth understanding of the cabinet's fluid dynamics.

CFD simulation was applied as a case study for a refrigeration cabinet. The simulation led to the conclusion that, for the lower shelves, the temperature is at least 4°C higher than the one required by standards, while there was a 6°C temperature difference between the upper and lower shelves of the cabinet; in the meantime, the simulation showed the non-uniformity of the air curtain in the vicinity of the base air grill. Turbulence intensity and temperature were higher at the back of the cabinet.

Nomenclature

A_1, A_2, A_3	amplitude of the air velocity functions, m/s
A_{11}, A_{22}, A_{33}	amplitude of the air temperature functions, °C
c	specific heat of the product, J/kg·°C
D_h	hydraulic diameter, m
h	convective heat transfer coefficient, W/m²·°C
I_t	turbulence intensity
m	product mass, kg
Re_{Dh}	Reynolds number based on the hydraulic diameter
S	product surface, m²
S_Φ	source term
T_1, T_2, T_3	period of the air velocity functions, s
T_{11}, T_{22}, T_{33}	period of the air temperature functions, s
t	product temperature, °C
t_i	initial product temperature, °C
t_f	final product temperature, °C
t_0	cooling medium temperature, °C
t_{1med}, t_{2med}, t_{3med}	average cabinet temperatures, °C

v	air velocity m/s
w	cooling rate, °C/s
x_i	orthogonal coordinates
α	relaxation factor
Γ_Φ	diffusion coefficient
ν	cinematic viscosity, m^2/s
ρ	density, kg/m^3
τ	time, s
τ_r	chilling time, s
ϕ	dependent variable

Author details

Radu Roşca*, Ioan Ţenu and Petru Cârlescu

*Address all correspondence to: rrosca@uaiasi.ro

University of Agricultural Sciences and Veterinary Medicine "Ion Ionescu de la Brad", Iaşi, Romania

References

[1] Mascheroni H M, editor. Operations in food refrigeration . Boca Raton, FL: CRC Press, Taylor&Francis Group; 2012. p. 383

[2] Sun Da-Wen, editor. Handbook of frozen food processing and packaging. Boca Raton, FL: CRC Press, Taylor&Francis; 2006. p. 723

[3] Fellows P. Food Processing Technology, principles and practice. 2nd edition. Cambridge: CRC Press, Woodhead Publishing Limited; 2000. p. 575

[4] Naghiu Al, Apostu S. Refrigeration and air conditioning techniques in food industry (in Romanian). Cluj-Napoca: 2006. p. 536

[5] James S J, James C. Meat refrigeration. Cambridge: CRC Press, Woodhead Publishing Limited; 2002. p. 347

[6] Singh R, Kachhwaha SS. Experimental studies on a scraped surface ice slurry generator. International Journal of Engineering Science and Innovative Technology. 2013;**2**(4):117–131. Available from: http://www.ijesit.com/Volume%202/Issue%204/IJESIT201304_18.pdf [Accessed: June 10, 2016]

[7]   IceSynergy. MaximICE Systems Information [Internet]. 2010. Available from: http://www.icesynergy.com/L2-4-2prod-syst.html [Accessed: 2017-01-20]

[8]   Graham J, Johnston WA, Nicholson FJ. Ice in fisheries. FAO Fisheries Technical Paper. 1992;**331**:75. Available from: http://www.fao.org/docrep/T0713E/T0713E00.htm#Contents [Accessed: May 21, 2016]

[9]   Funke. Heat Exchanger Systems [Internet]. 2016. Available from: http://en.funke.cn/products_detail/&productId=30.html [Accessed: 2017-01-20]

[10] Kennedy C J, editor. Managing frozen foods. Cambridge: CRC Press, Woodhead Publishing Limited; 2000. p. 286

[11] Faramarzi PER. Efficient display case refrigeration. ASHRAE Journal. 1999;**41**(11):46–54

[12] Fluent Incorporated. Fluent 6.1 User's Guide. Lebanon, New Hampshire: Fluent Incorporated; 2003. p. 1864